

Article

Micromachining of AlN and Al₂O₃ Using Fiber Laser

Florian Preusch, Benedikt Adelman * and Ralf Hellmann

Applied Laser and Phonics Group, University of Applied Sciences Aschaffenburg, Wuerzburger Strasse 45, D-63743 Aschaffenburg, Germany; E-Mails: florian.preusch@h-ab.de (F.P.); ralf.hellmann@h-ab.de (R.H.)

* Author to whom correspondence should be addressed; E-Mail: benedikt.adelmann@h-ab.de; Tel.: +49-602-1420-6840; Fax: +49-602-1420-6801.

External Editors: Maria Farsari and Costas Fotakis

Received: 12 August 2014; in revised form: 23 October 2014 / Accepted: 3 November 2014 /

Published: 10 November 2014

Abstract: We report on high precision high speed micromachining of Al₂O₃ and AlN using pulsed near infrared fiber laser. Ablation thresholds are determined to be 30 J/cm² for alumina and 18 J/cm² for aluminum nitride. The factors influencing the efficiency and quality of 3D micromachining, namely the surface roughness, the material removal rate and the ablation depth accuracy are determined as a function of laser repetition rate and pulse overlap. Using a fluence of 64 J/cm², we achieve a material removal rate of up to 94 mm³/h in Al₂O₃ and 135 mm³/h in AlN for high pulse overlaps (89% and 84%). A minimum roughness of 1.5 μm for alumina and 1.65 μm for aluminum nitride can be accomplished for medium pulse overlaps (42% to 56%). In addition, ablation depth deviation of the micromachining process of smaller than 8% for alumina and 2% for aluminum nitride are achieved. Based on these results, by structuring exemplarily 3D structures we demonstrate the potential of high quality and efficient 3D micromachining using pulsed fiber laser.

Keywords: ceramics; Al₂O₃; AlN; micromachining; fiber laser

1. Introduction

Micro structuring of materials with limited machinability by conventional machining methods, such as ceramics, can be executed by laser ablation employing pulsed lasers [1–3]. While, e.g., mechanical removal, electrical discharge machining, chemical or electrochemical treatment are less appropriate for

ceramics due to their high hardness, brittleness and chemical inertness, pulsed laser structuring evades these difficulties and combines the advantages of low mechanical stress, precision, process controllability and low thermal load. The latter being associated with a reduced heat affected zone surrounding the interaction zone of the laser impinging the processed specimen [4,5].

Technical ceramics such as Al_2O_3 and AlN are indispensable substrate materials for, e.g., microelectronics, electronic packaging and micro electro mechanical systems (MEMS) [5–7]. Their salient properties are a high electrical resistance, a high thermal conductivity and a great chemical resistance. With respect to their application in micro tooling, hot embossing dies for microfluidics, electronics and sensing both the ceramic micro structuring of the surface as well as the volume (3D structures) is of utmost importance [8]. Decreasing feature size and increasing requirements on quality and cost efficiency, expedite a further development of precise and efficient ablation processes with high removal rates and attainable surface roughness allowing the fabrication of complex 3D structures for, e.g., tooling inserts, to be fabricated [5]. Further quality aspects of the micro-structuring are spatial accuracy and steep ablated edges.

In case of ceramics, CO_2 lasers are primarily used for processes such as cutting, drilling and perforating [6,9]. For micro structuring, however, primarily pulsed solid state [4,10], and Excimer-lasers [11–13] have been applied with pulse durations in the nanosecond, picosecond and femtosecond regime. However, due to the substantial progress, also fiber lasers have recently been employed to efficiently process ceramics [4,14]. With regards to micromachining, fiber lasers offer a competitive edge by a high beam quality over their complete power range, a high reliability and long lifetime, as well as low operating costs. In addition, their compact design and inherent fiber delivery simplify the setup of workstations. Moreover, compared to CO_2 lasers, fiber lasers are capable to realize structures significantly smaller than $100\ \mu\text{m}$ in consequence of to a lower beam parameter product associated with the emission wavelength around $1\ \mu\text{m}$ [10].

With the focus on attainable surface roughness and processing speed, Sciti *et al.* utilized a KrF Excimer laser (248 nm) with pulse duration of 25 ns and fluences between 1.8 and $7.5\ \text{J}/\text{cm}^2$ to micro-structure unpolished Al_2O_3 [11]. A surface roughness R_a between 0.8 and $1.0\ \mu\text{m}$ was accomplished at a process rate between 1.0 and $2.0\ \text{mm}/\text{s}$. In addition, evidence was found that polished samples have a lower surface roughness R_a after laser treatment being on the order of 0.25 to $0.4\ \mu\text{m}$. Also using a KrF laser, Oliveira *et al.* worked on Al_2O_3 -TiC ceramics (fluence between 2 and $8\ \text{J}/\text{cm}^2$) and report on an increase of the surface roughness with increasing pulse number up to 200 pulses and an increase with fluence from $0.2\ \mu\text{m}$ at $2\ \text{J}/\text{cm}^2$ and $0.7\ \mu\text{m}$ at $8\ \text{J}/\text{cm}^2$, respectively [12].

Weichenhain *et al.* [10] deployed a frequency tripled pulsed diode-pumped solid-state laser (DPSSL) at $355\ \text{nm}$ with fluences between 1.9 and $16.2\ \text{J}/\text{cm}^2$ (pulse duration 10 ns, repetition rate 1 kHz) to process the non-oxide ceramics SiC and Si_3N_4 as a function of pulse overlap and fluence. For SiC the surface roughness remains almost constant at about $0.4\ \mu\text{m}$ for pulse overlaps up to 80%, being almost independent on fluence up to $16.2\ \text{J}/\text{cm}^2$. Ablating the material in different atmospheres (e.g., vacuum, ambient air, oxygen or nitrogen) does not significantly alter this behavior. Yet, above a pulse overlap of 80% the surface roughness raises sharply with an ambiguous dependence on fluence. For Si_3N_4 , however, the surface roughness reveals a more pronounced dependence on fluence also for low pulse overlaps with a varying behavior *versus* pulse overlap at different fluence levels. Moreover, the ambient gas atmosphere appears to have a stronger influence in case of Si_3N_4 as compared to SiC. A further discussion on the chemical composition of the treated surface upon laser irradiation in different

atmospheres is, however, not presented. Nonetheless, 3D micro geometries with feature sizes between 100 and 500 μm are generated to prove the concept of three dimensional micro structuring. To achieve high precision with low roughness and little residues, the process speeds had to be chosen below 10 mm/s with the fluence below 15 J/cm² [10].

A study on the near surface chemical composition after laser ablation of AlN by a KrF Excimer laser is presented by Hirayama *et al.* [9] using X-ray photoelectron spectroscopy. Examining the concentration depth profile within about 1.6 μm beneath the treated surface, it is shown that due to the nanosecond laser induced thermal decomposition process an aluminum layer is formed on the surface. Similar results are obtained using CO₂ lasers [6,9].

This contribution encompasses a study and optimization of the laser micro machining of Al₂O₃ and AlN using nanosecond fiber laser. The optimization targets high surface quality evaluated by the surface roughness and the accuracy of ablation depth for 3D volume ablation. As processing parameters the fluence, pulse overlap and laser repetition rate, respectively the process velocity, and the number of passes in a multi-pass process are varied. In addition, ablation thresholds and removal rates are determined and, finally, the distinguished quality of 3D micro structuring achievable with fiber laser is exemplified by realizing selected 3D structures.

2. Experimental Section

2.1. The Laser-System

For the experiments a pulsed 20 W fiber laser is used (YLP-1/100/20, IPG Photonics Corporation, Oxford, MA, USA), which is characterized by a pulse length of 100 ns, a beam quality of $M^2 = 1.6$ and an emission wavelength of 1064 nm. The repetition rate can be varied between 2 and 80 kHz with a nominal average power of 20 W at 20 kHz. The maximum pulse energy is 1 mJ and the maximum fluence is 64 J/cm² at a 44 μm spot diameter, respectively. While above 20 kHz the average power is constant with decreasing pulse energy at increasing repetition rate, below 20 kHz the average power decreases at constant pulse energy. At fixed repetition rate, the output power can get adjusted between 10% and 100% of the nominal power.

The laser beam is positioned over the specimen by a galvo scanner (Raylase SuperScan) with a focal length of 163 mm. The scanner deflects the laser spot over a square of 110 \times 110 mm² with a maximum positioning speed of larger than 7 m/s.

2.2. Materials

In this study, alumina and aluminum nitride with a purity of 96% and grain size of 3 to 5 μm (Ceramtec) are laser structured. The substrate platelets have a thickness of 0.33, 0.63 and 1 mm, respectively. Aluminum nitride has a specified thermal conductivity of 140 W/mK, alumina of 20 W/mK. For a spectral analysis of the absorption properties, we applied a spectroradiometer with equipped goniometer and integrating sphere in the detection arm to collect scattered light. For Al₂O₃, our measurements at room temperature reveal a reflection of 81% and a transmission of 16% at 1064 nm (substrate thickness 0.63 mm). This implies a calculated absorption of 3%. For AlN, the reflection is 44% and the transmission 12%, which yields an absorption of 44% (substrate thickness 1 mm).

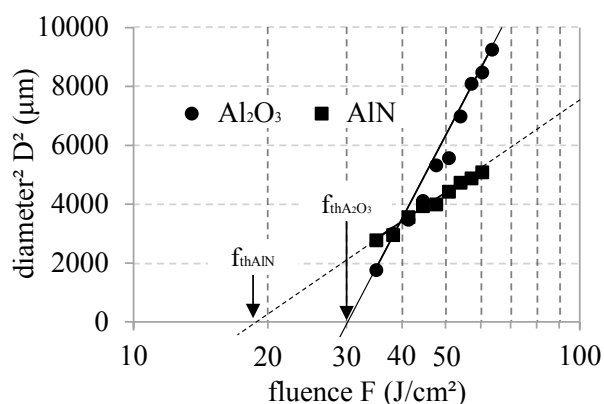
3. Results and Discussion

3.1. Ablation Threshold

In the conducted study, ablation of Al_2O_3 and AlN is initiated only for number of pulses. For instance, at a pulse repetition rate of 20 kHz ablation of Al_2O_3 requires about 1000 pulses. For comparative reasons, we therefore determine the ablation threshold fluence (F_{th}) for both materials for a sequence of 1000 pulses. For lasers having a Gaussian beam profile, F_{th} is typically determined by measuring the diameter of the generated ablation crater for varying fluences [15,16].

Figure 1 depicts the squared diameter of the ablation crater as measured by a confocal microscope versus the single pulse fluence in the center of the laser beam between 35 J/cm^2 and 64 J/cm^2 (fluence adjusted by changing the laser pulse energy, respectively the average power). According to [15], the intersection of a linear regression with the axis of abscissae (fluence), *i.e.*, a hypothetical vanishing crater diameter, yields the ablation threshold.

Figure 1. Squared diameters of Al_2O_3 and AlN as function of laser fluence.



For Al_2O_3 and AlN we determine an ablation threshold F_{th} of 30 and 18 J/cm^2 , respectively. The difference of F_{th} between Al_2O_3 and AlN in this study can be assigned to the different absorption of the materials at 1064 nm. Since ablation thresholds depend on, *e.g.*, the optical absorption that varies with wavelength [17,18] and on the number of pulses [19,20], F_{th} cannot be directly compared between different studies. In addition also the pulse length has an influence on the ablation threshold with by trend shorter pulses result in smaller thresholds [13]. Nonetheless, for a simplified assessment, the values found in this study correspond to those reported for CO_2 laser ablation [9]. In contrast, for excimer lasers, significantly lower ablation thresholds are determined in [9], which can be attributed to the higher absorption in the UV. Moreover, for femtosecond pulsed laser also lower threshold have been determined [21].

3.2. Correlation between Pulse Overlap and Roughness

For the application of micro structured ceramics, the surface roughness after laser ablation is of utmost importance. As previous studies have shown, it is strongly influenced by the pulse overlap [7,10]. Applying a meander type scanning strategy, we have investigated the surface roughness as a function of pulse repetition rate and pulse overlap of the laser scanning across the workpiece. The distance between two adjacent lines of the meander path is set equal to the distance between two following pulses within

one line. In addition, ablation is performed using the highest possible fluence of 64 J/cm² for high ablation rate and scanning the laser in five passes over an area of 1 × 1 mm². In addition, the pulse repetition rate is varied between 5 and 20 kHz.

Figure 2 shows the mean surface roughness R_a , measured by a laser scanning microscope, for alumina for different pulse overlaps between 42% and 89%. Below 42% pulse overlap, no material removal was observed for Al₂O₃. Please note, that the untreated alumina has a roughness R_a of 3.4 μm. After laser ablation, R_a is reduced to 1.50 μm at a pulse overlap of 42% and remains below the roughness of the untreated surface up to a pulse overlap of 56%. Between an overlap of 41% and about 80%, R_a increases independently of the repetition rate. Please note, that at constant pulse overlap an increase of the pulse repetition rate results in an equivalent increase of the velocity. For a pulse overlap exceeding 84%, the surface roughness increases sharply which is accompanied by an extended melt formation. A similar correlation between melt formation and roughness at high pulse overlap has been reported for laser structuring Y-TZP ceramics, being attributed to a hampered material ejection due to melt coverage [7].

In general, for AlN similar results are obtained as shown on Figure 3. However, due to the higher absorption material removal is already initiated at a pulse overlaps of 36%. Between 36% and 65% the surface roughness remains almost constant (R_a about 1.65 μm) and rises sharply for an overlap above of 80%. Yet, since AlN does not form a liquid phase [22], we associate this sharp increase with melt formation of liquid aluminum [9]. A comparable behavior, being explained by the presence of oxygen, has been observed by Weichenhain *et al.* when processing Si₃N₄ [10].

Figure 2. Mean roughness R_a as a function of pulse overlap at Al₂O₃.

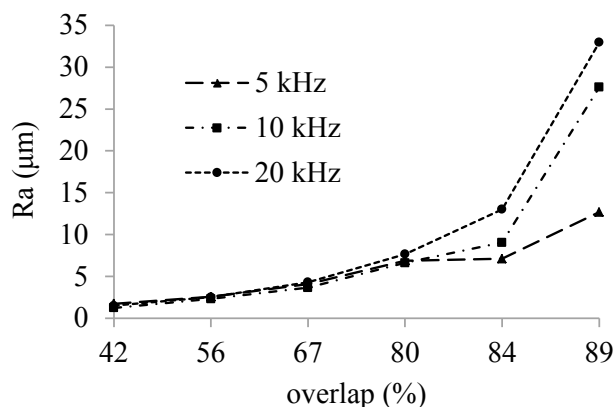
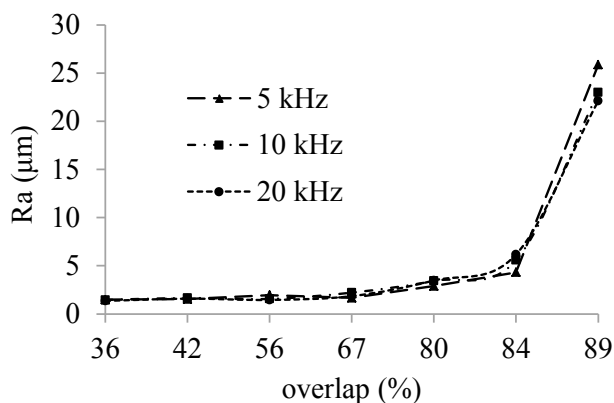


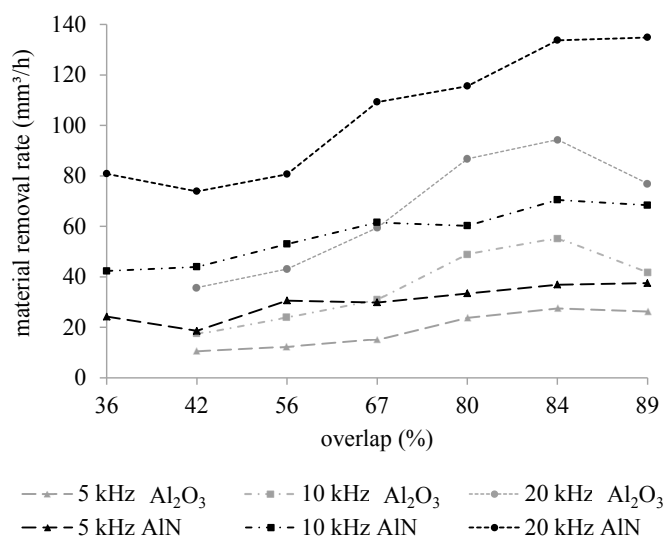
Figure 3. Mean roughness R_a as a function of pulse overlap at AlN.



3.3. Material Removal Rate

The removal rate is defined by the quotient of the ablated volume and the processing time. Figure 4 summarizes the removal rate for Al₂O₃ and AlN as a function of pulse overlap and for varying laser repetition rate. As a consequence of the lower ablation threshold for aluminum nitride, the removal rate of AlN is, in general, higher as compared to alumina. In particular, for alumina a maximum ablation rate of 94 mm³/h (84% pulse overlap, 20 kHz) and for aluminum nitride 135 mm³/h (89% pulse overlap, 20 kHz) is achieved.

Figure 4. Removal rate as a function of pulse overlap and for varying repetition rate for Al₂O₃ (grey line) and AlN (black line).



In addition, the removal rate increases for both pulse overlap and repetition rate. For example, in case of Al₂O₃ a maximum of 94 mm³/h is achieved for a pulse overlap of 84% at 20 kHz. This is significantly higher as compared to 10 mm³/h reported for laser ablation of alumina using a diode pumped solid state laser at a wavelength of 355 nm [23]. In addition, it is worthwhile to note that contrary to our findings in [23] the removal rate decreases with increasing pulse overlap. This can be attributed to the reduced absorption of the infrared fiber laser in the plasma that is generated during laser ablation. A higher plasma absorption in the UV reduces the energy input and thus the removal rate.

Since the laser pulse energy remains constant up to 20 kHz, an increase of pulse repetition rate corresponds to an increase of average laser power and consequently to a higher ablation rate (Figure 4).

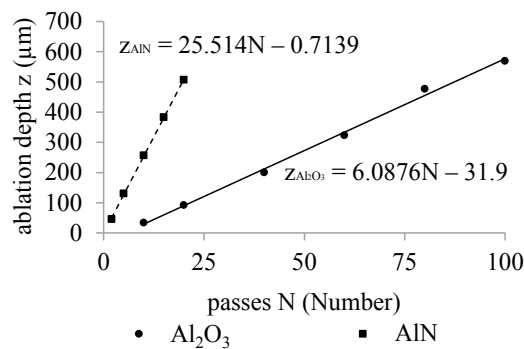
3.4. Ablation Depth Accuracy

For micromachining a 3D structure, the laser is scanned in a meander type pattern in multiple passes across the specimen until the targeted depth is achieved. For high quality 3D micromachining it is imperative to guarantee a high accuracy of the depth of ablation for multiple scan passes. In addition, a high material removal rate and a low surface roughness are desirable to ensure an efficient micromachining process and a high surface quality. To facilitate a good compromise between material removal rate and surface roughness, a fluence of 64 J/cm², a pulse overlap of 56% (Al₂O₃) and 77% (AlN) at a pulse repetition rate of 10 kHz are chosen to determine the depth of ablation accuracy. As each scan cycle

removes an equal amount of material with a depth of about 6 μm for Al₂O₃ and 25 μm for AlN, respectively, the total ablation depth can be varied with the number of passes.

Figure 5 reveals a linear dependence of the ablation depth as a function of the number of scan passes (meander type) for both alumina and aluminum nitride. The scanning velocities for these experiments are 200 mm/s for Al₂O₃ and 100 mm/s for AlN, respectively. Please note, that the linear regression does not intercept the origin of coordinates as for the first scan the ablation depth is smaller due to reduced absorption.

Figure 5. Removal rate as a function of pulse overlap and for varying repetition rate for Al₂O₃ (solid line) and AlN (dashed line).



Using the observed linear dependence, the number of required scan passes for a targeted ablation depth can be calculated. However, as this does not necessarily lead to an integer number, the number of scans has to be rounded up or down. As a result, the ablated depth deviates from the targeted value. Tables 1 and 2 compare the targeted, calculated and measured for a varying number of scans. Though the deviation between calculated and realized depth depends on the overall targeted depth and material, Table 1 highlights that the deviation is rather small, e.g., for AlN 1.5% for a targeted depth of 50 μm and <0.01% for a targeted depth of 500 μm. The reason for the higher accuracy of AlN ablation is assumed in the higher optical absorption compared to alumina which allows a more defined ablation. Based on this accuracy, high quality 3D structures can be realized in alumina and aluminum nitride.

Table 1. Comparison of targeted, calculated and measured ablation depth for Al₂O₃.

Characteristic	TARGET (μm)			
	50	100	300	500
number of passes (N)	14	22	55	87
calculated (μm)	53.3	102.0	302.9	497.7
measured (μm)	49.1	95.3	287.6	482.4
Deviation in %	7.9	6.6	5.0	3.0

Table 2. Comparison of targeted, calculated and measured ablation depth for AlN.

Characteristic	TARGET (μm)			
	50	100	300	500
number of passes (N)	2	4	12	20
calculated (μm)	50.3	101.3	305.5	509.6
measured (μm)	51.1	103.4	305.3	508.9
Deviation in %	1.5	2.0	<0.1	<0.1

4. Example of 3D Microstructures

Based on the experimental results presented above, defined 3D microstructures can be realized with high geometrical accuracy as well as high surface and edge quality. To prove the potential of fiber laser micromachining, Figure 6 depicts exemplarily an inversed pyramid realized in AlN that has been generated by sequentially ablating three squares having side lengths of 0.9, 0.6 and 0.3 mm and a depth of 300 μm per step. In contrast, Figure 7 illustrates a submerged pyramid in AlN, which has been realized by ablating seven steps with a depth of 100 μm each. For both microstructures an edge steepness between 70° and 75° is achieved.

Figure 6. Laser scanning microscope image of a fiber laser micro machined inverse pyramid in AlN.

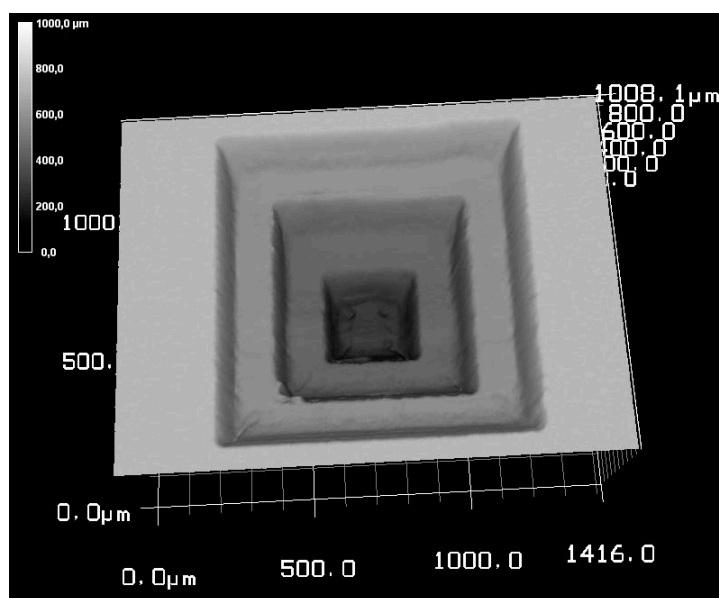
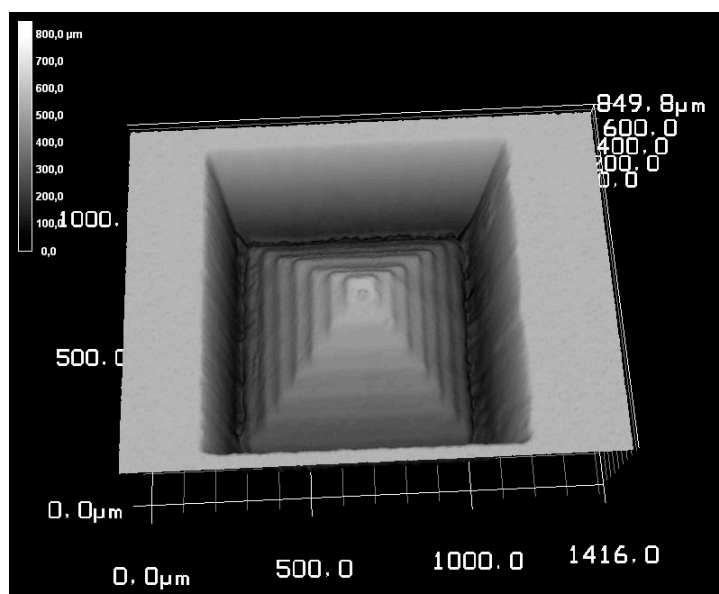


Figure 7. Laser scanning microscope image of a fiber laser micro machined submerged pyramid in AlN.



5. Conclusions

We have demonstrated that near infrared pulsed fiber lasers are eligible tools for efficient and high quality 3D micromachining. The pulse overlap and repetition rate are shown to be the most influencing parameters determining the achievable surface roughness and the material removal rate. The latter can be maximized for high repetition rates and overlaps, reaching a maximum of 94 mm³/h in Al₂O₃ and 135 mm³/h in AlN at a repetition rate of 20 kHz and pulse overlaps exceeding 84% and 89% for alumina and aluminum nitride, respectively. The surface roughness R_a can be minimized, however, for lower pulse overlaps being on the order of 50% reaching a level of 1.5 μm for Al₂O₃ and 1.65 μm for AlN. The ablation depth accuracy for multi-pass laser ablation is better than 8% for alumina and 2% for aluminum nitride, enabling high precision micro structuring.

Using a compromised parameter combination of maximum laser fluence (64 J/cm²), 10 kHz pulse repetition rate and medium pulse overlap (56% for Al₂O₃ and 77% for AlN) complex 3D structures in alumina and aluminum nitride are fabricated with high geometrical accuracy and high surface quality.

Acknowledgments

This contribution is funded by the Bavarian Research Foundation.

Author Contributions

Florian Preusch and Benedikt Adelman performed the experimental work, Ralf Hellmann is head of the Applied Laser and Photonics Group at the University of Aschaffenburg.

Conflicts of Interest

The authors declare no conflict of interest.

References

1. Kibria, G.; Doloi, B.; Bhattacharyya, B. Predictive model and process parameters optimization of Nd: YAG laser micro-turning of ceramics. *Int. J. Adv. Manuf. Technol.* **2013**, *65*, 213–229.
2. Knowles, M.R.H.; Rutterford, G.; Karnakis, D.; Ferguson, A. Micro-machining of metals, ceramics and polymers using nanosecond lasers. *Int. J. Adv. Manuf. Technol.* **2007**, *33*, 95–102.
3. Pham, D.T.; Dimov, S.S.; Petkov, P.V. Laser milling of ceramic components. *Int. J. Mach. Tools Manuf.* **2007**, *47*, 618–626.
4. Adelman, B.; Hellmann, R. Investigation on flexural strength during fiber laser cutting of alumina. *Phys. Procedia* **2013**, *41*, 398–400.
5. Samant, A.N.; Narendra, B.D. Laser machining of structural ceramics—A review. *J. Eur. Ceram. Soc.* **2009**, *29*, 969–993.
6. Molian, R.; Shrotriya, P.; Molian, P. Thermal stress fracture mode of CO₂ laser cutting of aluminum nitride. *Int. J. Adv. Manuf. Technol.* **2008**, *39*, 725–733.
7. Wang, X.; Shephard, J.D.; Dear, F.C.; Hand, D.P. Optimized Nanosecond Pulsed Laser Micromachining of Y-TZP Ceramics. *J. Am. Ceram. Soc.* **2008**, *91*, 391–397.

8. Vanko, G.; Hudek, P.; Zehetner, J.; Dzuba, J.; Choleva, P.; Kutiš, V.; Vallo, M. Rýger, I., Lalinský, T. Bulk micromachining of SiC substrate for MEMS sensor applications. *Microelectron. Eng.* **2013**, *110*, 260–264.
9. Hirayama, Y.; Yabe, H.; Obara, M. Selective ablation of ALN ceramic using femtosecond, nanosecond, and microsecond pulsed laser. *J. Appl. Phys.* **2001**, *89*, 2943–2949.
10. Weichenhain, R.; Horn, A.; Kreutz, E.W. Three dimensional microfabrication in ceramics by solid state lasers. *Appl. Phys. A* **1999**, *69*, 855–858.
11. Sciti, D.; Melandri, A.; Bellosi, A. Excimer laser-induced microstructural changes of alumina and silicon carbide. *J. Mater. Sci.* **2000**, *35*, 3799–3810.
12. Oliveira, V.; Vilar, R.; Conde, O. Excimer laser ablation of Al₂O₃—TiC ceramics: Laser induced modifications of surface topography and structure. *Appl. Surf. Sci.* **1998**, *127*, 831–836.
13. Ihlemann, J.; Wolff-Rottke, B. Excimer laser micro machining of inorganic dielectrics. *Appl. Surf. Sci.* **1996**, *106*, 282–286.
14. Shah, L.; Fermann, M.E.; Dawson, J.W.; Barty, C.P.J. Micromachining with a 50 W, 50 μJ, subpicosecond fiber laser system. *Opt. Express* **2006**, *14*, 12546–12551.
15. Liu, J.M. Simple technique for measurements of pulsed Gaussian-beam spot sizes. *Opt. Lett.* **1982**, *7*, 196–198.
16. Martin, S.; Hertwig, A.; Lenzner, M.; Krüger, J.; Kautek, W. Spot-size dependence of the ablation threshold in dielectrics for femtosecond laser pulses. *Appl. Phys. A* **2003**, *77*, 883–884.
17. Torrisi, L.; Borrielli, A.; Margarone, D. Study on the ablation threshold induced by pulsed lasers at different wavelengths. *Nucl. Instrum. Methods Phys. Res. Sect. B Beam Interact. Mater. At.* **2007**, *255*, 373–379.
18. Borowiec, A.; Tiedje, H.F.; Haugen, H.K. Wavelength dependence of the single pulse femtosecond laser ablation threshold of indium phosphide in the 400–2050 nm range. *Appl. Surf. Sci.* **2005**, *243*, 129–137.
19. Kautek, W.; Krüger, J.; Lenzner, M.; Sartania, S.; Spielmann, C.; Krausz, F. Laser ablation of dielectrics with pulse durations between 20 fs and 3 ps. *Appl. Phys. Lett.* **1996**, *69*, 3146–3148.
20. Stuart, B.C.; Feit, M.D.; Rubenchik, A.M.; Shore, B.W.; Perry, M.D. Laser-induced damage in dielectrics with nanosecond to subpicosecond pulses. *Phys. Rev. Lett.* **1995**, *74*, 2248.
21. Kim, S.H.; Sohn, I.k.; Jeong, S. Ablation characteristics of aluminum oxide and nitride ceramics during femtosecond laser micromachining. *Appl. Surf. Sci.* **2009**, *255*, 9717–9720.
22. Bengisu, M. *Engineering Ceramics*; Springer: Heidelberg, Germany, 2001.
23. Hellrung, D. Material Removal by Laser Radiation for the Fabrication of Three Dimensional Micro Molding Tools Made of Hard Materials. Ph.D. Thesis, RWTH Aachen University, Aachen, Germany, 2000. (In German)